Progressive Collapse Analyses of 2D Steel-Framed Structures with Different Connection Models

JOONHONG LIM and THEODOR KRAUTHAMMER

Progressive collapse has been an important issue in building failure characterization since the Ronan Point partial collapse (Griffiths, Pugsley, and Saunders, 1968). A gas explosion in the kitchen of an apartment on the 18th floor of the 22-story precast concrete panel construction building blew out an exterior wall panel. That caused a chain reaction of structural collapse of a corner of the building from the roof down to the ground level, as falling debris caused successive failures upon impact. The particular type of joint detail used in the Ronan Point building relied heavily on joint friction between elements, indicating that buildings with similar joint characteristics were particularly susceptible to progressive collapse (Breen, 1980).

Progressive collapse is a failure sequence that enhances local damage to cause large-scale collapse in a structure. The local failure can be defined as a loss of the load-carrying capacity of structural components that are part of the whole structure. Preferably, once any structural component fails, the structure should enable an alternative load-carrying path. After the load is redistributed through a structure, each structural component will be able to support the different load configuration. However, if any modified load exceeds the load-carrying capacity of a structural member, it will cause another local failure that will trigger another load redistribution. Such sequential failures can propagate through the structure. If a structure loses too many members, it may lead to a partial or total collapse. This type of collapse behavior may occur in buildings (Griffiths et al., 1968; Burnett, Somes, and Leyendecker, 1973; Ger, Cheng, and Lu, 1993; Sucuoğlu, Çitipitioğlu, and Altm, 1994; Ellis and Currie, 1998; Bazant and Zhou, 2002), trusses (Murtha-Smith, 1988; Blandford, 1997), and bridges (Ghali and Tadros, 1997; Abeysinghe, Gavaise, Rosignoli, and Tzaveas, 2002). Clearly, progressive collapse is an important structural phenomenon because uncontrolled local damage may evolve into a disproportionate failure of a structural system. Such undesired outcomes must be prevented since small accidents that cause localized damage cannot be avoided completely. Unfortunately, progressive collapse had not received much attention between the early 1970s and 2001, and its characteristics are not well understood. Investigating and understanding progressive collapse is essential for the development of safer structures. Current design guidelines for preventing progressive collapse [for example, GSA (2003) and DOD (2005)] were developed before this phenomenon had been comprehensively studied. Initial local damage is defined in these guidelines as a sudden removal of a single column, without other damage to the remaining structural system. Obviously, such "clean" local damage involving a single column is very unlikely [for example, Krauthammer (2003)], and this definition simplifies the required analyses. Although structures are three-dimensional (3D) systems and both the GSA and DOD guidelines recommend 3D analyses, such treatment is not explicitly required. Furthermore, the use of nonlinear dynamic analyses tools is also not required. Actually, in both guidelines various illustrations imply a two-dimensional (2D) treatment of localized damage. Obviously, when the design-level analyses can be carried out in simplified 2D approach, designers might not address the more complicated 3D nonlinear dynamic aspects of the problem. Therefore, one needs to assess the differences between 2D and 3D considerations of failure and progressive collapse.

Krauthammer, Lim, Choi, and Elfahal (2004) addressed various aspects of progressive collapse behavior. They studied numerically, with several computer codes, single-column buckling, and two-dimensional (2D) and three-dimensional (3D) frames with various combinations of spans and stories with rigid, semi-rigid, and reinforced semi-rigid connections. This paper is dedicated to validating the numerical treatment of single-column buckling analyses with different computer codes and the numerical analyses of 2D frames with different combinations of spans, stories, connection types, and initial local damage. That initial effort focused on buildings of up to five stories high, and up to 5x5 bays. After the completion of the initial study, the research has continued with follow-up studies of much larger buildings that reached up to 20 stories. The follow-up effort is aimed at the development of fast-running computational assessment tools

Joonhong Lim is a structural engineer, WSP Cantor Seinuk, New York, NY.

Theodor Krauthammer is professor, department of civil and environmental engineering, Penn State University, Protective Technology Center, State College, PA.

to support the mitigation of progressive collapse. A similar effort has been reported by Hansen, Wong, Lawver, Oneto, Tennant, and Ettouney (2005).

BEHAVIOR AND FAILURE CAUSES

Progressive collapse may occur in any type of framed structures, and it is not necessarily related to any one type of structural material. However, some types of materials may be more prone to progressive collapse in that they may have less ductility or have weaker connection details than others (Breen and Siess, 1979). The causes of progressive collapse of steel frames may be several, as follows (Christiansson, 1982):

1. Material failure due to high stresses.
2. Failure as a result of the inability of the structure to sustain the large deformations.
3. Stability failure of the entire structure.
4. Local stability failure in the form of buckling, etc.

Christiansson (1982) noted that there is no sharp distinction between Causes 1 and 2. Cause 1 applies mainly to a brittle material, while Cause 2 may occur when the deformation capacity of the material has been exhausted. Similarly, he stated that there is no sharp distinction between Causes 3 and 4. Consequently, one may reconsider only two categories, material and buckling failures.

Additionally, there is another important failure case in steel framed structures. It is a connection failure. For example, many buildings were damaged due to the Northridge earthquake. It turned out that connections were damaged in more than 200 buildings (Whittaker, Gilani, and Bertero, 1998; Joh and Chen, 1999). It is very common practice to use a rigid or pinned connection between steel members for analysis purposes. However, experiments have shown that a real steel connection is neither rigid nor pinned (Kameshki and Saka, 2003). Furthermore, experiments have also shown that when a moment is applied to a ductile connection, the relationship between the moment and the beam-column rotation is nonlinear (Kameshki and Saka, 2003), as shown in Figure 1.

A connection should be considered as an individual member of the structure when its behavior is semi-rigid. Axial and rotational springs can be adopted to simulate the behavior of a semi-rigid nonlinear connection. Here, only rotational nonlinear springs will be used to simulate a semi-rigid connection, assuming that the moment-curvature relationship of a semi-rigid connection dominates its behavior, as shown in Figure 2.

ADVANCED ANALYSIS

Advanced analysis refers to any method of analysis that represents the strength and stability behavior such that separate specification member capacity checks are not required (Chen and Toma, 1994). The main distinction between advanced analysis and other simplified analysis methods is that advanced analysis combines, for the first time, the theories of plasticity and stability in the limit states design of structural steel frameworks. Other analysis and design methods treat stability and plasticity separately—usually through the use of beam-column interaction equations and member effective length factors (Liew, White, and Chen, 1991).

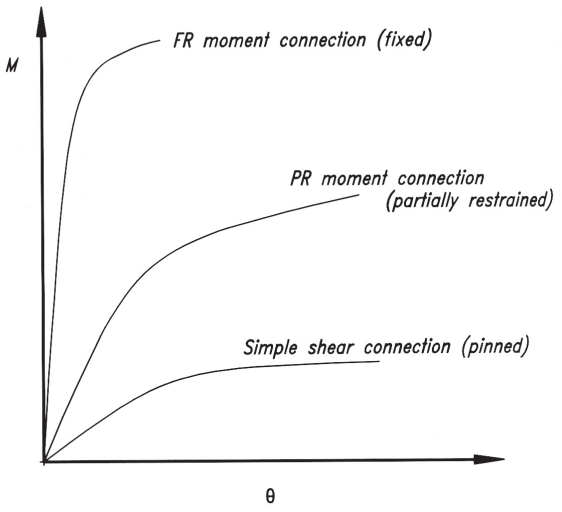

Fig. 1. Moment-curvature curves (AISC, 1994).

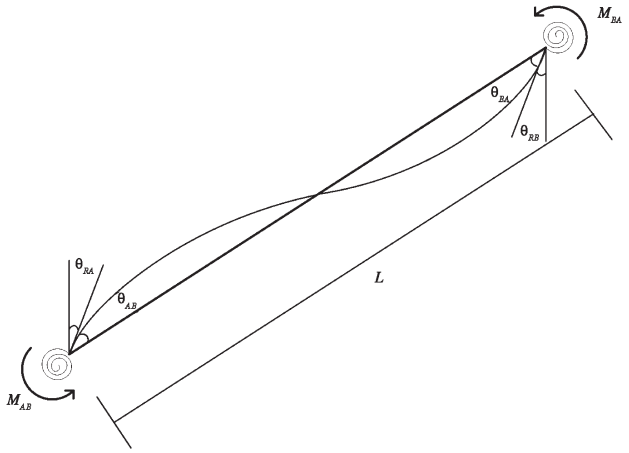

Fig. 2. Semi-rigid plane member.

When a change in the geometry of a structure or structural component under compression will result in the loss of its ability to resist loadings, this condition is called instability. Equilibrium equations must be written based on the geometry of the structure that becomes deformed under load. This is known as a second-order analysis (Chen and Lui, 1987). The stiffness of a structure changes as the geometry changes. If the load and deformation keep changing or increasing, the stiffness of a structure may reach a point of stiffness vanishing, and buckle. In ordinary structural analysis, the original geometry does not change even if the load reaches an extreme value. Therefore, ordinary structural analysis cannot capture the buckling phenomenon.

There is another issue called inelastic buckling (Salmon and Johnson, 1996). Euler's theory pertains only to situations where the compressive stress below the elastic limit acts uniformly over the cross section when buckling failure occurs. However, in many cases, some fibers in the cross section yield when the member buckles. This is called inelastic buckling. If all fibers in the cross section yield before the member reaches its critical load, it is called material failure. Inelastic buckling is affected by strength and stability, simultaneously. Therefore, a second-order inelastic analysis is required to achieve an advanced analysis.

Clarke developed a plastic-zone using the total Lagrangian formulation and Newton-Raphson method (Chen and Toma, 1994). In Clarke's finite element nonlinear formulation, a curved line element was used. The element stiffness matrices and nodal residual force vectors were integrated numerically along the element length using three-point Gaussian quadrature. A commercial finite element code, ABAQUS (Hibbitt, Karlsson, and Sorensen, 2002a, 2002b), was selected to perform the advanced analysis in this study because it has the ability to implement a second-order inelastic analysis. The ability of this computer code to simulate inelastic buckling was validated by comparing results from single-column analyses with the result derived by Clarke (Chen and Toma, 1994; Krauthammer et al., 2004).

SEMI-RIGID CONNECTION

A semi-rigid connection transfers part of the moment in the beam to the column. Moment-curvature relationships for semi-rigid connections are usually nonlinear, as shown in Figure 1. The nonlinear characteristics of beam-to-column connections play a very important role in frame resistance and stability, because semi-rigid connections enable larger story drift than rigid connections. This ability of larger story drifts influences the P–Δ effect, which can lead to column buckling.

It is necessary to know the moment-curvature behavior of semi-rigid connections to analyze the frame accurately. At present, the most commonly used approach to describe the moment-curvature relationship is to curve-fit experimental data with simple expressions (Chen and Toma, 1994). Frye and Morris (1975) reported a polynomial model to evaluate the behavior of several types of connections. Lui and Chen (1986) used an exponential function to curve-fit experimental moment-curvature data. Kishi and Chen (Chen and Toma, 1994) refined the Lui-Chen exponential model to accommodate any sharp slope changes in the moment-curvature relationship. Richard and Abbot (1975) proposed a power model using three parameters: initial connection stiffness, ultimate moment capacity, and shape parameters, as shown by the following generalized equation

$$M = \frac{R_{ki}\theta_r}{\left\{1+\left(\frac{\theta_r}{\theta_0}\right)^n\right\}^{1/n}} \tag{1}$$

where

R_{ki} = initial connection stiffness

θ_0 = a reference plastic rotation (M_u/R_{ki})

M_u = ultimate moment capacity

n = shape parameter

Figure 3 shows the moment-curvature curves for various shape parameter values, n. From this figure, it is recognized that the larger the power index, n, the steeper is the curve.

The power model is an effective tool for designers to execute a second-order nonlinear structural analysis, because the tangent connector stiffness, R_k, and relative rotation, θ_r, can be determined directly from Equation 1 without iteration, as follows

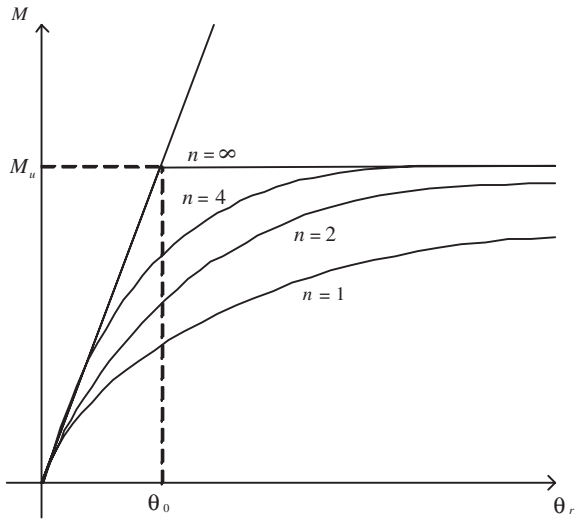

Fig. 3. Three-parameter power model.

$$R_k = \frac{dM}{d\theta_r} = \frac{R_{ki}}{\left\{1+\left(\frac{\theta_r}{\theta_0}\right)^n\right\}^{(n+1)/n}} \tag{2}$$

and the rotation, θ_r, is

$$\theta_r = \frac{M}{R_{ki}\left\{1-\left(\frac{M}{M_u}\right)^n\right\}^{1/n}} \tag{3}$$

Kishi and Chen (1990) proposed a method to determine these parameters using a simple mechanical procedure with an assumed failure mechanism. Based on their previous work, Kishi, Chen, Goto, and Matsuoka (1993) presented a practical design procedure that uses angles for the connection. In that paper, the initial connection stiffness, R_{ki}, the ultimate moment capacity, M_u, and the shape parameter, n, of the three-parameter power model can be determined easily. The top and seat angle with double web angle connection was chosen in this study to simulate semi-rigid connection behavior. The design procedures are as follows.

Assumptions and Notations

t = angle thickness

k = gage distance from heel to the top of fillet

l = angle length

g = distance between heel to the center of fastener closest to beam web or flange

W = nut width

I_0 = $t^3/12$ = geometrical moment of inertia, per unit length of plate element of angle

M_0 = $\sigma_y t^2/4$ = pure plastic bending moment, per unit length of plate element of angle

σ_y = yielding stress of steel

The top and seat angle are assumed to have the same dimensions.

The following parameters were also used:

$$\beta = \frac{g}{l},\ \gamma = \frac{l}{t},\ \delta = \frac{d}{t},\ \kappa = \frac{k}{t},\ \omega = \frac{W}{t},\ \rho = \frac{t_w}{t_t}$$

d = height of beam

where subscripts t and w denote top angle and web angle, respectively.

Top and Seat Angle without Double Web Angle Connection

Assuming that the center of rotation is located at the angle leg adjacent to the compression beam flange, and the top angle acts as a cantilever beam to resist surcharged moment, the initial connection stiffness, R_{kits}, is obtained as follows (Kishi and Chen, 1990)

$$\frac{R_{kits}}{EI_{0t}} = (1+\delta_t)^2 D_{ts} \tag{4}$$

where

$$D_{ts} = \frac{3}{\beta_t'(\gamma_t^2\beta_t'^2 + 0.78)} \tag{5}$$

$$\beta_t' = \beta_t - \frac{1+\omega_t}{2\gamma_t} \tag{6}$$

The ultimate capacity, M_{uts}, is obtained by assuming a simple failure mechanism. The equation for M_{uts} is given by the following expression

$$\frac{M_{uts}}{M_{0t}t_t} = \gamma_t\left\{1+\xi_t\left[1+\beta_t^* + 2(\kappa_t+\delta_t)\right]\right\} \tag{7}$$

where the variable ξ_t is a nondimensional ultimate shearing force acting at the plastic hinge. As in the case of single web angle connections, it is obtained by solving the following equation

$$\xi_t^4 + \beta_t^*\xi_t - 1 = 0 \tag{8}$$

where

$$\beta_t^* = \beta_t'\gamma_t - \kappa_t \tag{9}$$

Top and Seat Angle with Double Web Angle Connection

The initial connection stiffness, R_{ki}, and the ultimate moment capacity, M_u, can be determined by separating the top and seat angle part and the double web angle part, as follows:

$$\frac{R_{ki}}{EI_{0t}} = \frac{R_{kits}}{EI_{0t}} + \frac{R_{kiw}}{EI_{0t}} \tag{10}$$

$$\frac{M_u}{M_{0t}t_t} = \frac{M_{uts}}{M_{0t}t_t} + \frac{M_{uw}}{M_{0t}t_t} \tag{11}$$

As for the web angle, it acts as a cantilever beam similar to the behavior of the top angle, and the initial connection stiffness, R_{kiw}, is related to the double web angle connection part, as follows (Kishi and Chen, 1990)

$$\frac{R_{kiw}}{EI_{0t}} = (1+\delta_t)^2 \rho D_w \tag{12}$$

where

$$D_w = \frac{3}{2\beta'_w(\gamma_w^2 \beta'^2_w + 0.78)} \tag{13}$$

β_w' is defined the same as β_t' in Equation 6.

In the limit state, the ultimate moment capacity, M_{uw}, is obtained by choosing a simple failure mechanism of the web angle and taking moment about the center of rotation at the angle leg adjacent to the compression beam flange, as follows

$$\frac{M_{uw}}{M_{0t}t_t} = \gamma_w(1+\xi_w)\left\{\frac{\xi_w - 1}{3(\xi_w+1)}\gamma_w + \delta_w + \frac{1}{\rho}\right\}\rho^3 \tag{14}$$

where ξ_w can be obtained by solving the following equation

$$\xi_w^4 + (\beta_w\gamma_w - \kappa_w)\xi_w - 1 = 0 \tag{15}$$

Determination of Parameters in the Power Model

The only parameter that is not determined in the three-parameter power model of Equation 1 is the shape parameter, n. The equation to determine the shape parameter n was given by Kishi et al. (1993), as follows:

1. If $\log_{10}\theta_0 > -2.880$, then $n = 2.003 \log_{10}\theta_0 + 6.070$ (16)

2. If $\log_{10}\theta_0 \le -2.880$, then $n = 0.302$ (17)

Rotational Capacity of Joint Connection

A rotational capacity of a joint connection is obtained from its moment-rotation relationship, as shown in Figure 4. Here, M_u is the ultimate moment capacity of the joint, R_{ki} is the initial connection stiffness, and θ_u is the theoretical elastic rotation magnitude, determined as follows

$$\theta_u = \frac{M_u}{R_{ki}} \tag{18}$$

The rotational capacity of a joint can be obtained by a multiple of θ_u, such that the total rotation becomes $k\theta_u$. The actual magnitude of k may vary, depending on the design code requirement. In this study, a k value of 6 was chosen, on the premise that this would be satisfactory for all but the most severe seismic requirement (Bjorhovde, Brozzetti, and Colson, 1990).

CODE VALIDATION—SINGLE COLUMN ANALYSES

As noted earlier, inelastic buckling is a central parameter in progressive collapse analysis, and any numerical approach considered for simulating such behavior must be able to reproduce it. Therefore, one must validate that the computer codes adopted or developed for this study can represent this physical behavior. It is possible to calculate the critical load of a member with the Euler buckling load equation. However, this equation is only valid if the member is slender enough. If the member is relatively short, fibers in the cross section would yield before the load reaches the critical buckling load, as explained previously. There are several strength curves that can compensate for the slenderness of columns (Salmon and Johnson, 1996). The strength curves that were provided by AISC (AISC, 1994) were used for comparison purposes, because these curves were derived based on well-accepted theoretical and experimental efforts.

Three computer codes were used in this study to analyze and compare the buckling behavior of a single column. They are ABAQUS/Standard (Hibbitt et al., 2002a), ABAQUS/Explicit (Hibbitt et al., 2002b), and nonlinear frame analysis (NFA) that was developed in this study based on Clarke's formulation (Chen and Toma, 1994). ABAQUS/Standard is a commercial finite element software package that uses an implicit integration method, while ABAQUS/Explicit uses an explicit integration method.

The selected member for the calculations had a W12×106 cross section. The geometry of a W12×106 cross section and the load configuration are shown in Figure 5.

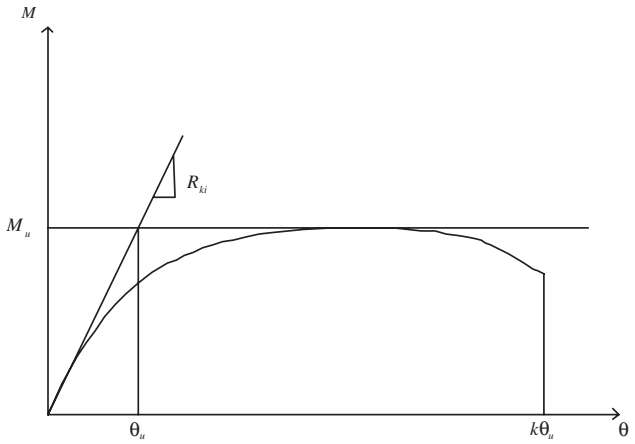

Fig. 4. Rotational capacity of joint connection.

The column was assumed to be fixed at the bottom and free at the top. Therefore, the effective length factor, *K*, is 2.0. The column length, *l*, was adjusted to achieve slenderness ratios between 20 and 200, so that the second-order effect and material failure can be clarified. A horizontal force *P/n* was applied at the top of the column to provide the eccentric load, where *n* is given as 1,000, 500, 200, 100, and 50. The modulus of elasticity and yield stress of the column were assumed as 2.9×10^7 psi (2.0×10^5 MPa), and 3.6×10^4 psi (248 MPa), respectively. The plastic behavior of the model was elastic-perfectly plastic. Each simulated column was composed of three 2-node linear beam elements. The results for three cases are compared and discussed herein, and additional information is provided in Krauthammer et al. (2004).

Slenderness Ratio: 20
[Column Length: 54.7 in. (1.39 m)]

A column that has a slenderness ratio of 20 is very short. It was expected that this column would crush (in other words, material failure) when the load approached its critical state.

With the smallest eccentric load (*P*/1,000), all cases showed that the column failed at the LRFD critical load. As the eccentric load increased, each column failed at a lower load. All failures occurred suddenly when the cross section reached the yield stress. Therefore, the second-order effect in the short column was not significant, as expected.

Figure 6 shows a comparison of the results from the three different computer codes. The results are virtually the same for the smallest eccentric load. However, ABAQUS/Explicit showed a different slope for the biggest eccentric load

$$P/50\,\frac{n!}{r!(n-r)!}$$

ABAQUS/Standard and NFA showed very close results. It seems that differences between the explicit and implicit algorithms were responsible for these results. However, these cases have almost the same critical load, regardless of their slope differences.

Slenderness Ratio: 100
[Column Length: 273.5 in. (6.95 m)]

Figure 7 shows the column behavior for a slenderness ratio of 100. This column was no longer short, and the Euler buckling load approached the LRFD critical load. Since the LRFD critical load considered both the initial crookedness of the column and the eccentric load effects, the LRFD critical load was still lower than the Euler buckling load.

The nonlinear behavior of the columns became clear in this region, because the second-order effect was activated. The displacement increased rapidly, as the load approached the critical value, and Figure 7 shows that the results from the three computer codes matched well.

Slenderness Ratio: 200
[Column Length: 547.0 in. (13.90 m)]

The results for the column with a slenderness ratio of 200 are shown in Figure 8. It is noted that a small eccentric critical load approached the Euler buckling load (in other words, elastic buckling load). The critical loads with the smallest eccentric load (*P*/1,000) from ABAQUS/Explicit and ABAQUS/Standard exceeded the Euler buckling load by 7.2 and 4.7%, respectively. However, the critical load obtained with NFA and with the smallest eccentric load (*P*/1,000) approached the Euler buckling load. It seems that the difference in the number of monitoring points in the cross section

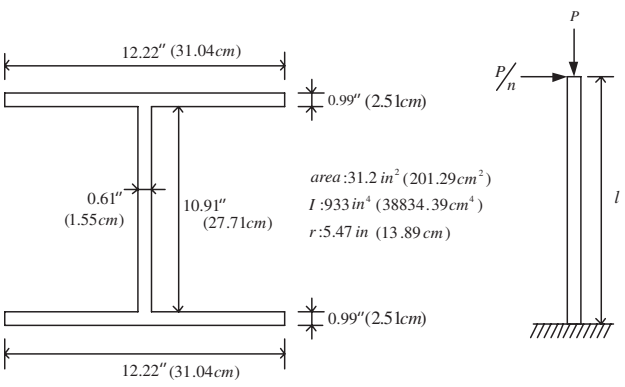

Fig. 5. Geometry and load configuration of W12×106 column.

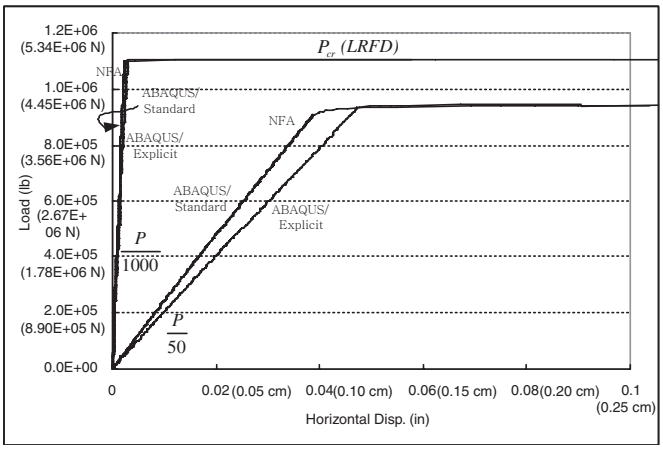

Fig. 6. Single column behavior at slenderness ratio 20.

caused different results. The number of monitoring points in ABAQUS (Explicit and Standard) is only five, while NFA has 45 monitoring points. However, the results from ABAQUS (Explicit and Standard) are still reasonable. Besides, the horizontal displacement obtained with ABAQUS/Explicit reached almost 15 in. when the load was at the Euler buckling load.

These results show that all three computer codes provided reasonably accurate solutions, as compared with the Euler buckling load and the LRFD critical load. Therefore, since ABAQUS (Explicit and Standard) have the ability to handle both second-order and material nonlinearity effect, these codes can be adopted to analyze more complicated 2D and 3D frame structures. Consequently, ABAQUS/Explicit was chosen for this study.

2D FRAME ANALYSES

Sixteen frames were used for the 2D simulations, and their dimensions are shown in Figure 9. The 2D frame analyses were performed for several combinations of numbers of spans and stories. The frames ranged from 2x2 spans to 5x5 spans, and up to five stories high. All spans were 24 ft (7.315 m) long; columns were 12 ft (3.657 m) high and based on the AISC *LRFD Manual of Steel Construction* (AISC, 1994). Each analysis included second-order and material nonlinearity effects with different connection stiffnesses to study their possible effects on failure and progressive collapse. The initial localized failure (in other words, single column removal) was assumed for the outside column of the first floor. The external loads were self weight and typical office loads. The gravity acceleration was given as 386 in./sec^2 (9.8 m/sec^2), and a typical office load was 50 lbs/ft^2 (2.39 kPa). Analyses were performed for up to 7 seconds after the initial failure.

The moment curvature relationships of the connections were calculated based on the procedure discussed previously, as shown in Figure 10. The failure rotation was 0.0192 radian, the initial stiffness was 2.311×10^8 lb-in./rad (2.611×10^7 N-m/rad). Each beam had a W12×26 cross section. Column sizes depend on the number of stories in each frame, as shown in Figure 9. The influence of the floor slab was ignored because the strength of the floor slab is not considered in the ordinary design process. The Young's modulus of structural steel is 2.9×10^7 psi (2.0×10^5 MPa) and the yield stress is 3.6×10^4 psi (248 MPa).

Rigid Frames

A rigid connection transfers all moments in the beams and the columns to the adjacent structural members. Figure 11 shows the total collapse of the 5x4 span rigid frame, and Figure 12 shows the partial collapse of the 5x5 span rigid frame. The 5x5 span frame shows an interesting result. The failure of this frame was localized to the first span above the initial column failure. However, the previous 5x4 frame showed a total collapse. Therefore, it may imply that the column design in the 5x5 frame is more robust than in the 5x4 frame, so that the horizontal failure propagation will not be initiated.

Table 1 shows the collapse summary of the rigid frames analyzed in this study. As the number of spans increased, the collapse mode changed from total collapse to partial collapse. As the number of stories increased, the collapse mode changed from the partial collapse to total collapse except, in the 5x5 span frame. Clearly, a frame structure exhibited better survival if it had more spans and fewer stories.

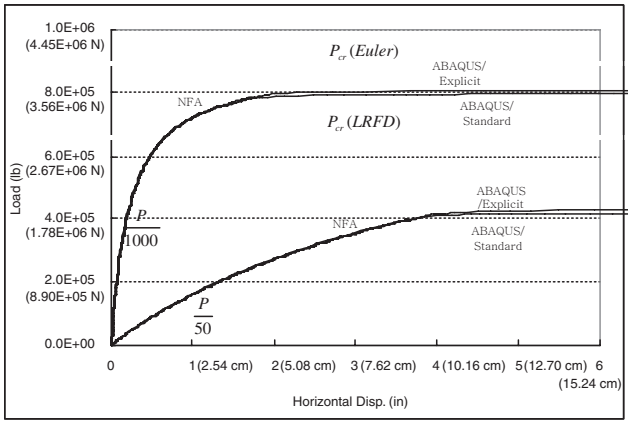

Fig. 7. Single column behavior at slenderness ratio 100.

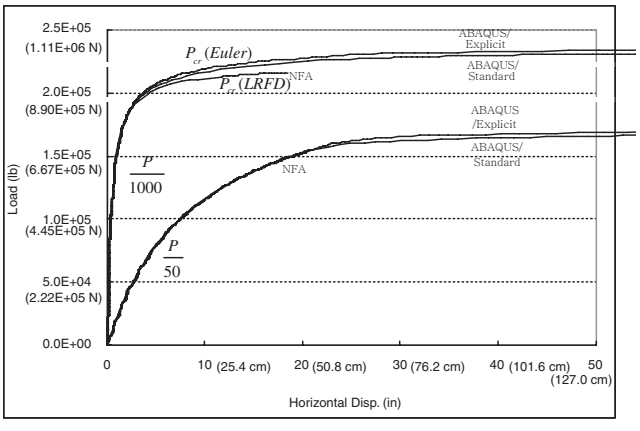

Fig. 8. Single column behavior at slenderness ratio 200.

Table 1. Collapse Modes of Rigid Frames

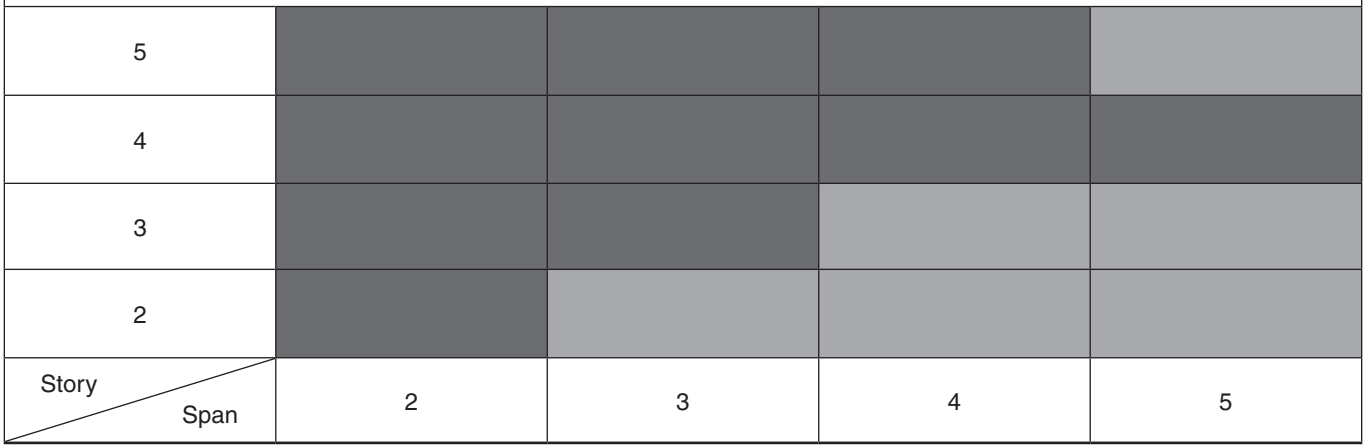

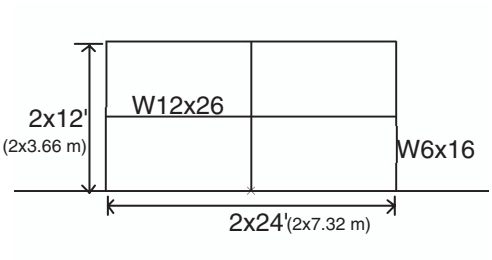

(a) 2×2 Span Frame

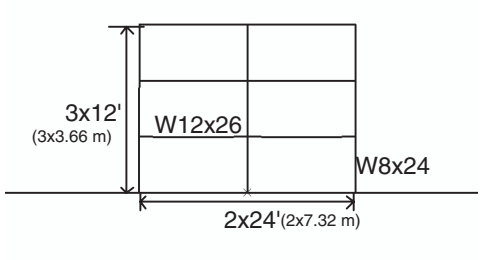

(b) 2×3 Span Frame

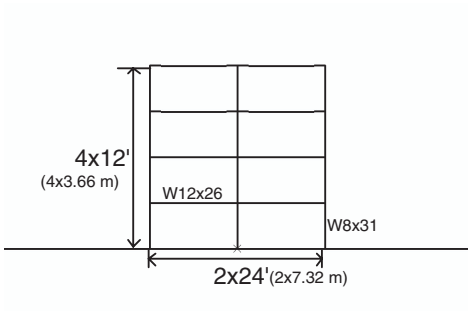

(c) 2×4 Span Frame

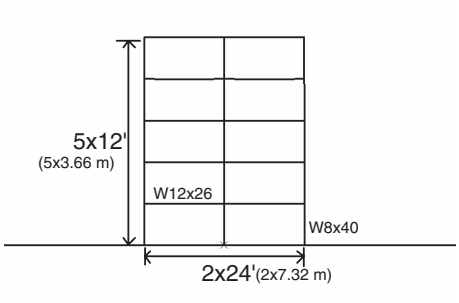

(d) 2×5 Span Frame

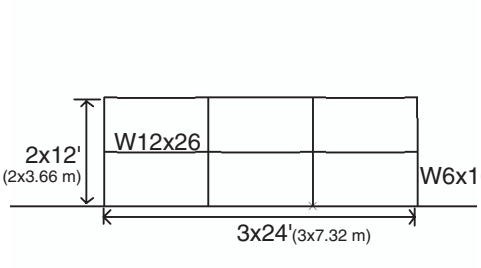

(e) 3×2 Span Frame

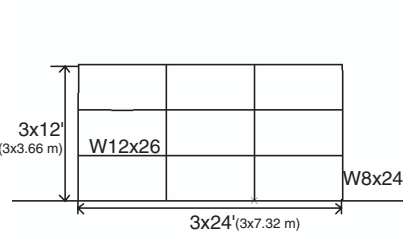

(f) 3×3 Span Frame

Fig. 9. Dimensions of the 2D frames.

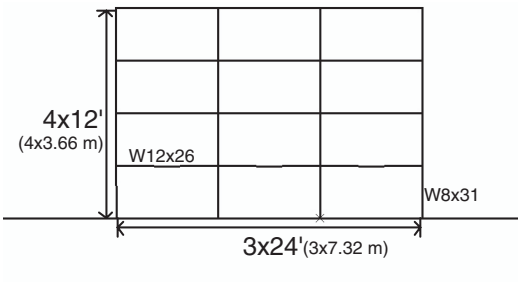

(g) 3×4 Span Frame

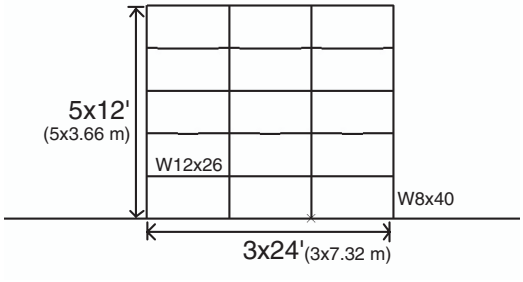

(h) 3×5 Span Frame

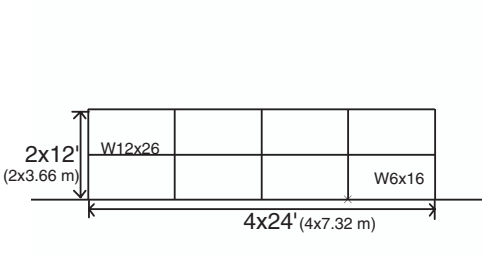

(i) 4×2 Span Frame

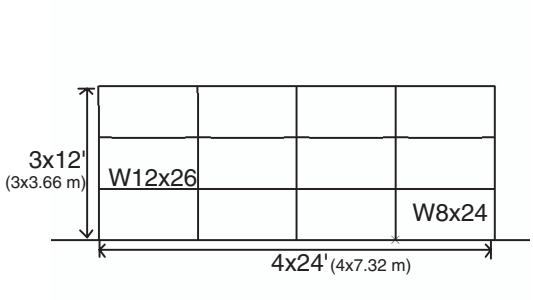

(j) 4×3 Span Frame

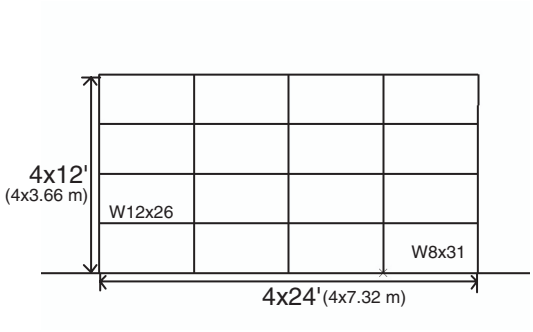

(k) 4×4 Span Frame

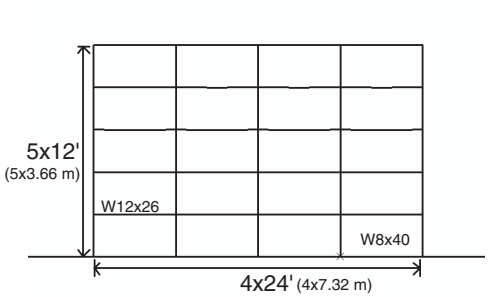

(l) 4×5 Span Frame

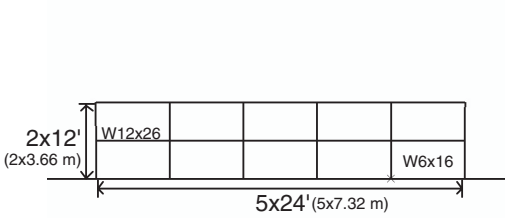

m) 5×2 Span Frame

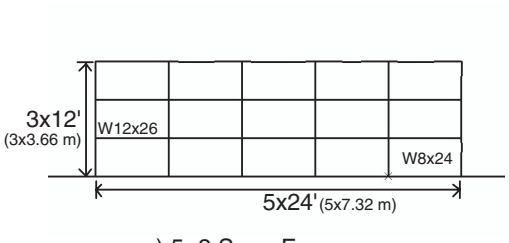

n) 5×3 Span Frame

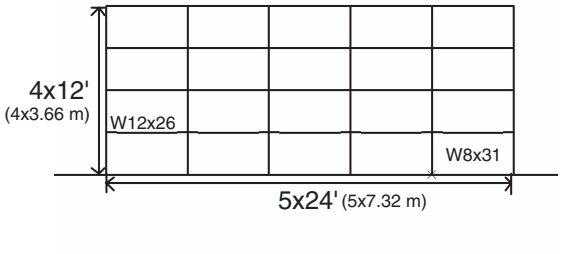

(o) 5×4 Span Frame

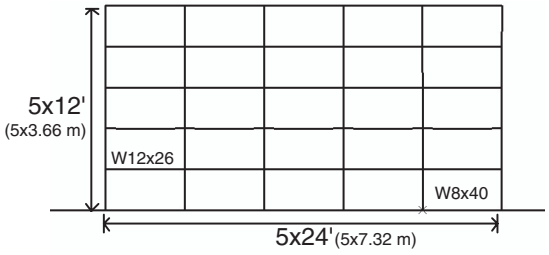

(p) 5×5 Span Frame

Fig. 9 (continued). Dimensions of the 2D frames.

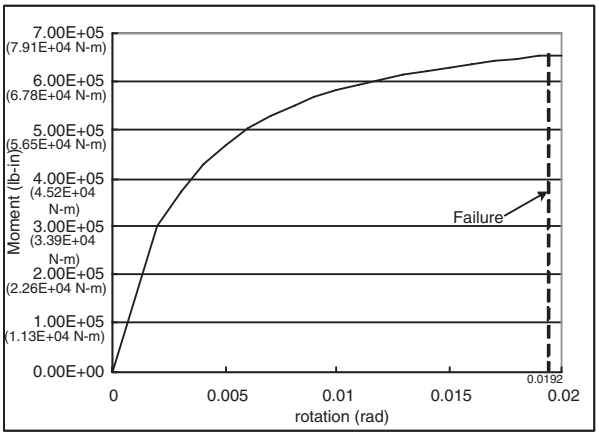

Fig. 10. Moment curvature relationship of the semi-rigid connection.

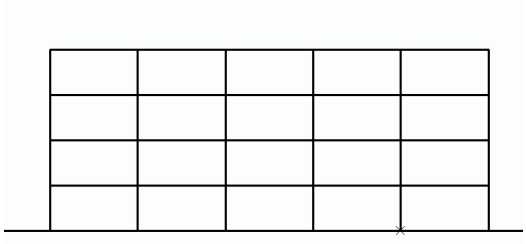

(a) Before Initial Failure

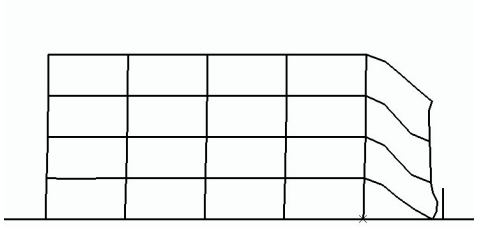

(b) Vertical Failure (1.15 sec)

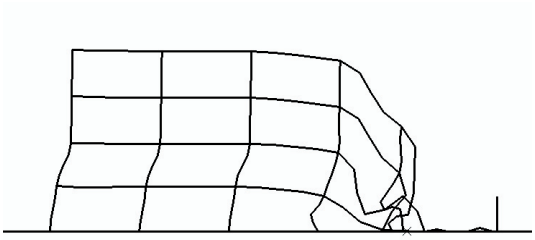

(c) Horizontal Failure (5.35 sec)

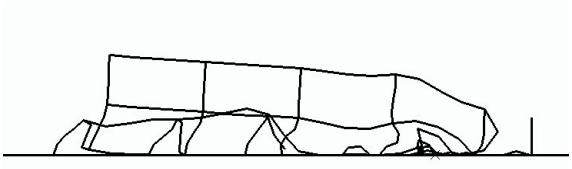

(d) Total Failure (7.00 sec)

Fig. 11. Total collapse of the 5x4 rigid frame.

Semi-Rigid Frames

An assumption of rigid connections is used to simplify the analysis, and it could be reasonable for ordinary design situations. However, since progressive collapse considerations require one to define accurately the expected behavior, one should consider the effects of deformable connections. Semi-rigid connections enable nonlinear behavior and the ability to characterize failure more accurately. Therefore, it should be very important to include the behavior of semi-rigid connections in progressive collapse analyses. Figure 13 shows the partial collapse of the 5x5 semi-rigid frame.

All semi-rigid frames collapsed partially because of joint connection failure. However, only the first span above the initial column failure collapsed. The collapse was limited to a local area, and this failure mode was different from the failure modes that were noted in the rigid frames.

Reinforced Semi-Rigid Frames

Various semi-rigid frames with reinforced joints were analyzed to study the possible effect of connection reinforcement. The moment capacities of each joint were increased between two and five times, respectively, as shown in Figure 14. However, to simplify the analysis, the same rotational capacity was used.

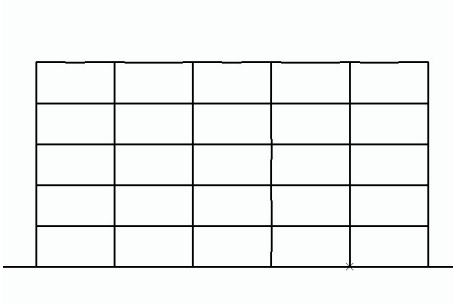

(a) Before Initial Failure

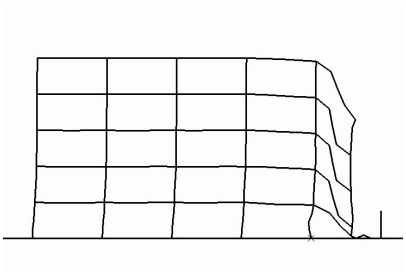

(b) Final Failure (2.20 sec)

Fig. 12. Partial collapse of the 5x5 rigid frame.

The results for these cases are presented in Table 2. The results show that the failure mode approached the rigid frame cases as the joint resistance increased. The responses of the four-times reinforced semi-rigid frame were almost the same as the responses of the rigid frames. It shows that if a rigid frame is required, joint connection resistances should be enhanced by a factor of four, as compared to the ordinary joint (a factor of one) design.

Table 2(a) shows the trend of partial collapse due to connection failures. This collapse mode is dominated by the connections rigidities. The entire semi-rigid frame with connection resistance enhanced by a factor of two, collapses in this mode. Three quarters of the three-times and only two cases of the four-times resistance enhanced frames collapsed in this mode. This failure mode disappears completely if the connection is enhanced by more than four times.

However, the total collapse mode appears as the joint is more reinforced, as shown in Table 2(b), as was noted for the rigid frames. This collapse mode dominates for strong connections in frames with higher stories, and for frames with strong connections and fewer stories and spans. Since this failure mode is undesirable, it is not always a good idea to over reinforce the connection. Table 2(c) shows cases that exhibited partial collapse with damage. If some level of collapse is inevitable, the partial collapse option is the best choice. This failure mode dominated when frames had a few stories and many spans (in other words, low-rise frames). In the cases studied here, this failure mode did not appear for more than four-story frames, except in the 5x5 frame.

CONCLUSIONS

It was observed in this study that the collapse modes of the 2D frame structures depended on various factors, such as the geometries, material properties, loads, and especially connection rigidity. Rigid frames were assumed in many previous studies for simplicity, and they provided good solutions for ordinary behavioral conditions. However, there is no guarantee that the rigid joint assumption can provide realistic solutions for severe cases, such as blast, earthquake, and progressive collapse, as was noted elsewhere (Whittaker et al., 1998; Joh and Chen, 1999). Therefore, various joint rigidities were used for this study.

Combinations of several numbers of stories and spans with connection showed that the collapse modes depended on the number of stories and spans. As the number of spans increased, the collapse mode changed from total collapse to partial collapse. As the number of stories increased, the collapse mode changed from partial collapse to total collapse. Therefore, rigid frame structures can survive better with more bays and fewer stories. This observation might be expressed as follows:

$$\frac{n_{span}}{n_{story}} \leq 1 \quad \text{for total collapse of low-rise rigid 2D frames} \tag{19}$$

$$\frac{n_{span}}{n_{story}} > 1 \quad \text{for partial collapse with damage of low-rise rigid 2D frames} \tag{20}$$

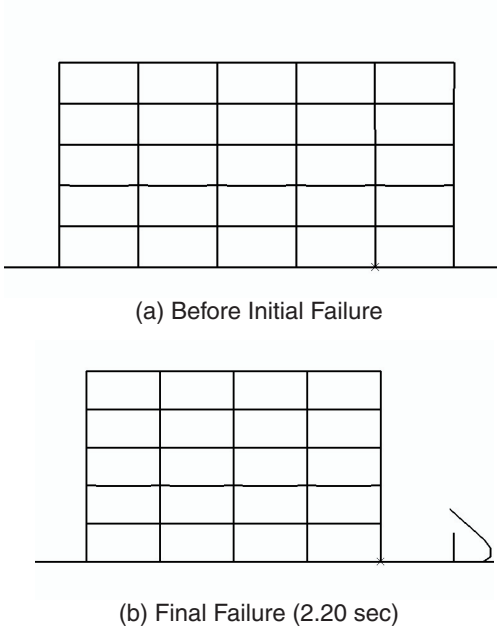

Fig. 13. Partial collapse of the 5x5 semi-rigid frame.

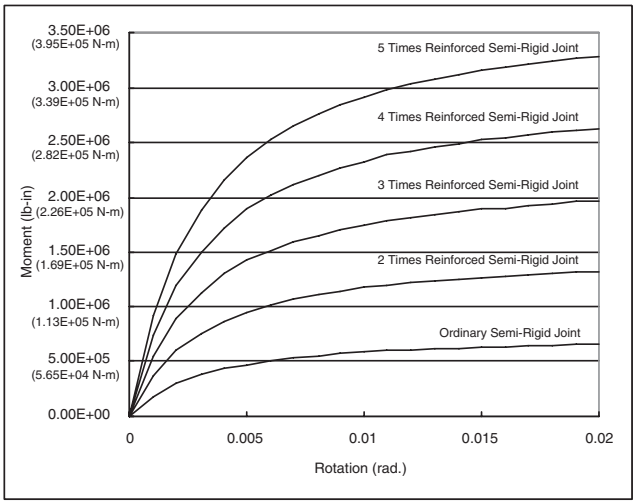

Fig. 14. Joint moment-curvature relationships of the frames.

Table 2. Collapse Modes by Various Semi-Rigid Connections
(a) Partial Collapse by Connection Failure

Story	Span	Ordinary Frame	2 Times Reinf. Frame	3 Times Reinf. Frame	4 Times Reinf. Frame	5 Times Reinf. Frame	Rigid Frame
2	2	■	■				
	3	■	■				
	4	■	■				
	5	■	■	■			
3	2	■	■				
	3	■	■	■			
	4	■	■	■	■		
	5	■	■	■	■		
4	2	■	■	■			
	3	■	■	■			
	4	■	■	■			
	5	■	■	■			
5	2	■	■	■			
	3	■	■	■			
	4	■	■	■			
	5	■	■	■			

(b) Total Collapse

Story	Span	Ordinary Frame	2 Times Reinf. Frame	3 Times Reinf. Frame	4 Times Reinf. Frame	5 Times Reinf. Frame	Rigid Frame
2	2			■	■	■	■
	3			■			
	4			■			
	5						
3	2			■	■	■	■
	3				■	■	■
	4						
	5						
4	2				■	■	■
	3				■	■	■
	4				■	■	■
	5				■	■	■
5	2				■	■	■
	3				■	■	■
	4				■	■	■
	5				■	■	

No Collapse

Collapse

Table 2 (continued). Collapse Modes by Various Semi-Rigid Connections
(c) Partial Collapse with Damage

Story	Span	Ordinary Frame	2 Times Reinf. Frame	3 Times Reinf. Frame	4 Times Reinf. Frame	5 Times Reinf. Frame	Rigid Frame
2	2						
	3						
	4						
	5						
3	2						
	3						
	4						
	5						
4	2						
	3						
	4						
	5						
5	2						
	3						
	4						
	5						

No Collapse

Collapse

In which n_{span} is the number of spans and n_{story} is the number of stories. If the inequality (19) is valid, low-rise 2D rigid frames may collapse totally. If the inequality (20) is valid, low-rise rigid 2D frames may collapse partially with damage.

However, the analyses of the semi-rigid frames showed different results. All semi-rigid frames collapsed partially by joint failure. The collapse was limited to the local zone, where only the first bay above the initial column failure collapsed all the way to the ground. Since the joints failed before all moments and forces were transferred to the adjacent members, the horizontal failure propagation did not occur. Therefore, it is possible to prevent the whole frame collapse with ordinary semi-rigid joint design and to sacrifice only the bay with the failed span.

These two extreme cases may indicate that there would be transitional collapse modes if the stiffnesses of the joint varied between semi-rigid and rigid. Table 2 shows that the collapse trends were divided into partial collapse by connection failure, total collapse, and partial collapse with damage. It shows that ordinary and two-times reinforced semi-rigid frames collapsed due to connection failure. As the joints became stronger, this collapse mode disappeared. The total collapse mode appeared with a more than four-times reinforced connection. The results of a four-times reinforced connection are similar to those of the rigid frames. Partial collapse with damage also appeared in this range. This collapse mode occurred when frames had fewer stories and many spans. It seems that this collapse mode would disappear for a frame with more than four stories, if a sufficient number of bays exist.

The best result is, of course, no damage after the initial failure. However, it may not be possible to guarantee such an outcome because of the nature of abnormal loadings. Therefore, it seems that damage propagation control might be the best strategy to consider in a design.

The second best damaged case is the partial collapse with damage. It happened in frames with a few stories or many spans with strong or rigid joints. However, strong or rigid joints can cause total collapse, if the frame has too many stories or too few bays. Ordinary semi-rigid connections can be used for that situation. Such connections can act as circuit

breakers. They could disconnect members when subjected to abnormal loads, stop transferring moments and forces, and prevent failure propagation. However, it can also cause total destruction of the failed span. Therefore, the use of mixed connection types should be considered carefully. Besides, specific responses can change if the geometry, material properties, and external loads are different.

Most of all, these progressive collapse analyses have shown that once failure propagation (in other words, horizontal column buckling) was initiated, it would not stop until it caused total collapse (or almost total collapse). Therefore, control of horizontal column buckling propagation is the key parameter to prevent progressive collapse.

ACKNOWLEDGMENTS

The authors acknowledge the generous support for this study by the Defense Threat Reduction Agency (DTRA) and the U.S. Army Engineer Research and Development Center (ERDC).

REFERENCES

Abeysinghe, R.S., Gavaise, E., Rosignoli, M., and Tzaveas, T. (2002), "Pushover Analysis of Inelastic Seismic Behavior of Greveniotikos Bridge," *Journal of Bridge Engineering*, Vol. 7, No. 2, March, pp. 115–126.

AISC (1994), *Load and Resistance Factor Design Manual of Steel Construction*, 2nd ed., American Institute of Steel Construction, Inc., Chicago, IL.

Bazant, Z.P. and Zhou, Y. (2002), "Why Did the World Trade Center Collapse?—Simple Analysis," *Journal of Engineering Mechanics*, Vol. 128, No. 1, January, pp. 2–6.

Bjorhovde, R., Brozzetti, J., and Colson, A. (1990), "A Classification System for Beam to Column Connections," *Journal of Structural Engineering*, Vol. 116, No. 11, pp. 3059–3076.

Blandford, G.E. (1997), "Review of Progressive Failure Analyses for Truss Structures," *Journal of Structural Engineering*, Vol. 123, No. 2, February, pp. 122–129.

Breen, J.E. and Siess, C.P. (1979), "Progressive Collapse—Symposium Summary," *ACI Journal*, September, pp. 997–1004.

Breen, J.E. (1980), "Developing Structural Integrity in Bearing Wall Buildings," *PCI Journal*, January–February.

Burnett, E.F.P., Somes, N.F., and Leyendecker, E.V. (1973), "Residential Buildings and Gas-Related Explosions," Center for Building Technology Institute for Applied Technology National Bureau of Standards, Washington, D.C.

Chen, W.F. and Lui, E.M. (1987), *Structural Stability—Theory and Implementation*, Prentice Hall.

Chen, W.F. and Toma, S. (1994), *Advanced Analysis of Steel Frames*, CRC Press.

Christiansson, P. (1982), "Steel Structures Subjected to Dynamic Loads in Connection with Progressive Collapse. Dynamic Buckling," Swedish Council for Building Research, Stockholm, Sweden.

DOD (2005), *Design of Building to Resist Progressive Collapse*, Unified Facilities Criteria (UFC), UFC 4-023-03, Department of Defense, 25 January.

Ellis, B.R. and Currie, D.M. (1998), "Gas Explosions in Buildings in the UK: Regulation and Risk," *Structural Engineer*, Vol. 76, No. 19, October.

Frye, M.J. and Morris, G.A. (1975), "Analysis of Flexibly Connected Steel Frames," *Canadian Journal of Civil Engineering*, pp. 280–291.

Ger, J., Cheng, F.Y., and Lu, L. (1993), "Collapse Behavior of Pino Suarez Building During 1985 Mexico City Earthquake," *Journal of Structural Engineering*, Vol. 119, No. 3, February, pp. 852–870.

Ghali, A. and Tadros, G. (1997), "Bridge Progressive Collapse Vulnerability," *Journal of Structural Engineering*, Vol. 123, No. 2, February, pp. 227–231.

Griffiths, H., Pugsley, A., and Saunders, O. (1968), "Collapse of Flats at Ronan Point, Canning Town," Her Majesty's Stationery Office, London.

GSA (2003), "Progressive Collapse Analysis and Design Guidelines for New Federal Office Buildings and Major Modernization Projects," General Services Administration, June.

Hansen, E., Wong, F., Lawver, D., Oneto, R., Tennant, D., and Ettouney, M. (2005), "Development of an Analytical Database to Support Fast Running Progressive Collapse Assessment Tool," *Proceedings, 2005 Structures Congress and 2005 Forensic Engineering Symposium*, American Society of Civil Engineering, New York, NY, April, pp. 20–24.

Hibbitt, Karlsson and Sorensen (2002a), "ABAQUS/Standard User's Manual v. 6.3," Hibbitt, Karlsson & Sorensen, Inc.

Hibbitt, Karlsson, and Sorensen (2002b), "ABAQUS/Explicit User's Manual v. 6.3," Hibbitt, Karlsson & Sorensen, Inc.

Joh, C. and Chen, W. (1999), "Fracture Strength of Welded Flange-Bolted Web Connections," *Journal of Structural Engineering*, May, pp. 565–571.

Kameshki, E.S. and Saka, M.P. (2003), "Genetic Algorithm Based Optimum Design of Nonlinear Planar Steel Frames with Various Semi-Rigid Connections," *Journal of Con-*

structional Steel Research, Vol. 59, pp. 109–134.

Kishi, N. and Chen, W.F. (1990), "Moment-Rotation Relations of Semi-Rigid Connections with Angles," ASCE, *Journal of Structural Engineering,* pp. 1813–1834.

Kishi, N., Chen, W.F., Goto, Y., and Matsuoka, K.G. (1993), "Design Aid of Semi-rigid Connections for Frame Analysis," *Engineering Journal*, Vol. 30, No. 3, 3rd Quarter, pp. 90–107.

Krauthammer, T. (2003), "AISC Research on Structural Steel to Resist Blast and Progressive Collapse," *Proceedings, AISC Steel Building Symposium: Blast and Progressive Collapse Resistance*, December, New York, NY.

Krauthammer, T., Lim, J., Choi, H., and Elfahal, M. (2004), "Evaluation of Computational Approaches for Progressive Collapse and Integrated Munitions Effects Assessment," PTC-TR-002-2004, Protective Technology Center, Pennsylvania State University, June.

Liew, J.Y.R., White, D.W., and Chen, W.F. (1991), "Beam-Column Design in Steel Frameworks—Insight of Current Methods and Trends," *Journal of Constructional Steel Research*, Vol. 18, pp. 269–308.

Lui, E.M. and Chen, C.F. (1986), "Analysis and Behavior of Flexibly Jointed Frames," *Engineering Structures*, pp.107–118.

Murtha-Smith, E. (1988), "Alternate Path Analysis of Space Trusses for Progressive Collapse," *Journal of Structural Engineering*, Vol. 114, No. 9, September, pp. 1978–1999.

Richard, R.M. and Abbott, B.J. (1975), "Versatile Elastic-Plastic Stress-Strain Formula," *Journal Engineering Mechanical Division*, ASCE, Vol.101, No. EM4, pp. 511–515.

Salmon, C.G. and Johnson, J.E. (1996), *Steel Structures/ Design and Behavior*, 4th ed., Harper Collins College Publishers.

Sucuoğlu, H., Çitipitioğlu, E., and Altm, S. (1994), "Resistance Mechanisms in RC Building Frames Subjected to Column Failure," *Journal of Structural Engineering*, Vol. 120, No. 3., March, pp. 765–782.

Whittaker, A., Gilani, A., and Bertero, V. (1998), "Evaluation of Pre-Northridge Steel Moment-Resisting Frame Joints," *The Structural Design of Tall Buildings*, pp. 263–283.